Romanian Reports in Physics, Vol. 65, No. 1, P. 103–113, 2013

ELEMENTARY PARTICLE PHYSICS

PRECISION MEASUREMENT OF THE PROTON STRUCTURE AT HERA*

N. RAIČEVIĆ ON BEHALF OF THE H1 AND ZEUS COLLABORATIONS

University of Montenegro, Faculty of Science, Džordža Vašingtona BB, 81000 Podgorica, Montenegro, E-mail: raicevic@mail.desy.de

Received September 12, 2012

Abstract. The H1 and ZEUS collaborations work on precision measurements of the proton structure at the HERA $e^{\pm}p$ collider. To achieve high precision measurements, data from both experiments have been combined leading to significantly reduced experimental uncertainties. The most recent results of combined measurements from $e^{\pm}p$ deep inelastic scattering are reported and their impact on understanding the proton structure is discussed.

Key words: Deep Inelastic Scattering (DIS), cross-section, structure functions, neutral current, charged current, charm, DGLAP, parton density function (PDF).

1. INTRODUCTION

Deep inelastic scattering (DIS) of leptons off nucleons has been crucial for our knowledge of the internal structure of the nucleon. The world's only electron/positron-proton collider, HERA at DESY, has had a great impact in revealing details of the partonic structure of the proton. The large center-of-mass energy of $\sqrt{s}$ = 319 GeV allowed an extension of the available phase space by two orders of magnitude both in Q^2, the negative four-momentum transfer squared, and the Bjorken scaling variable x compared with previous fixed-target DIS experiments. The maximum value of Q^2 reaches almost 10^5 GeV^2, which corresponds to a spatial resolution of 10^{-16} cm. The minimum x, which represents the momentum fraction carried by the struck parton in the proton's infinite momentum frame, reaches down to almost 10^{-5}.

* Paper presented at the 8th General Conference of Balkan Physical Union, July 5–7, 2012, Constanța, Romania.

During a period of 15 years of data taking, the H1 and ZEUS collaborations at HERA successfully operated their general purpose detectors. The data taken until the year 2000, with electron/positron beam energy 27.6 GeV and proton beam energies 820, 920 GeV (HERA-I period), have provided accurate neutral current and charged current DIS cross section measurements from about 200 pb^{-1} of e^+p and about 30 pb^{-1} of e^-p scattering data per experiment. In 2001, HERA and the detectors were upgraded to reach higher luminosities (HERA-II period). Until March 2007, HERA provided about 500 pb^{-1} of $e^{\pm}p$ collisions to each of the experiments. From March to June 2007, HERA performed a series of dedicated runs with reduced proton beam energies of 460 and 575 GeV, as compared to the nominal one of 920 GeV, for a direct measurement of the longitudinal proton structure function.

HERA data are of crucial importance in constraining the parton density functions (PDFs) of the proton. H1 and ZEUS are now working together, combining their results and performing common QCD analysis in order to provide data and proton PDFs with the highest possible accuracy.

2. DIS CROSS SECTIONS AND PDFS

The reduced cross section of the neutral current (NC) DIS interaction, mediated by γ and Z exchange, $e^{\pm} + p \rightarrow e^{\pm} + X$, can be written as,

$$\sigma_{NC}^{r}(e^{\pm}p) = \frac{\mathrm{d}^2\sigma_{NC}(e^{\pm}p)}{dxdQ^2} \cdot \frac{xQ^4}{2\pi\alpha^2 Y_+} = F_2 \mp \frac{Y_-}{Y_+} xF_3 - \frac{y^2}{Y_+} F_L , \qquad (1)$$

where α is the fine structure constant. The helicity dependence of the electroweak interactions is given by the terms $Y_{\pm} = 1 \pm (1 - y)^2$ with y being the inelasticity which represents the energy transfer between the lepton and the hadron system in the proton rest frame. F_2, xF_3 and F_L are the structure functions of the proton. In the framework of the perturbative QCD inspired quark parton model, the structure functions can be directly related to the parton density functions which are probability densities of partons existing inside the proton. At low Q^2, F_2 is the dominant contribution to the cross section which is an electric-charge squared weighted sum of the quark and anti-quark PDFs of all flavours. In the low x region, F_2 is dominated by sea-quark PDFs, and the DGLAP [1] evolution of QCD ascribes the Q^2 dependence of F_2 ("scaling violation") due to gluons splitting into quark-anti-quark pairs. The HERA experiments provide crucial information on the small-x sea-quark and gluon PDFs. At low Q^2, the contribution of Z exchange is negligible and xF_3=0. At large values of Q^2, xF_3 becomes significant, and gives

information about the valence quark distributions, $u_v = u - \bar{u}$ and $d_v = d - \bar{d}$. The longitudinal structure function, F_L, is zero in the quark-parton model, *i.e.* without QCD, but in leading order QCD, a finite value of F_L is expected in the small x region by being directly related to the gluon PDF. The contribution of the term containing the longitudinal structure function in (1) is only significant for high y.

The reduced cross section of the charged current (CC) DIS interaction, mediated by W^+ and W^- exchange, $e^+(e^-) + p \to \bar{\nu}(\nu) + X$, can be written as,

$$\sigma^r_{CC}(e^\pm p) = \frac{4\pi x}{G_F^2} \cdot \frac{(Q^2 + M_W^2)^2}{M_W^4} \cdot \frac{\mathrm{d}^2\sigma_{CC}(e^\pm p)}{\mathrm{d}x\mathrm{d}Q^2}, \tag{2}$$

with G_F being the Fermi coupling constant and M_W the mass of the exchanged W boson. The CC reduced cross sections are expressed *via* quark and anti-quark distribution functions,

$$\sigma^r_{CC}(e^+ p) \sim x\bar{U} + (1-y)^2 xD = (x\bar{u} + x\bar{c}) + (1-y)^2 (xd + xs), \tag{3}$$

$$\sigma^r_{CC}(e^- p) \sim xU + (1-y)^2 x\bar{D} = (xu + xc) + (1-y)^2 (x\bar{d} + x\bar{s}). \tag{4}$$

The $e^\pm p$ NC and CC cross sections can therefore be written completely in terms of up-type, $xU = x(u + c)$, down-type, $xD = x(d + s)$, and anti-quark type, $x\bar{U} = x(\bar{u} + \bar{c})$ and $x\bar{D} = x(\bar{d} + \bar{s})$, distributions. These (anti-)quark distributions can be determined from HERA data alone. This has the advantage that there is no need for heavy target corrections, which must be applied to the fixed target data which are used in the global PDF fits, and isospin asymmetry assumption, that d in the proton is the same as u in the neutron, since information on the distribution can be obtained directly from CC e^+p.

3. COMBINATION OF H1 AND ZEUS MEASUREMENTS

In order to provide the most complete and accurate set of deep-inelastic data as the legacy of HERA, the H1 and ZEUS experiments began to combine their data in 2008. The cross section measurements from neutral and charged current interactions from the HERA-I running period were combined and this combination was used for the extraction of the HERAPDF1.0 NLO parton density functions [2]. The combination of the H1 and ZEUS data sets takes into account the full correlated systematic uncertainties of the individual experiments such that the total uncertainty of the combined measurement for $3 < Q^2 < 500$ GeV^2 is typically smaller than 2%, and reaches 1%, for $20 < Q^2 < 100$ GeV^2.

3.1. HERA-II INCLUSIVE DATA SETS AT HIGH Q^2

The combined HERA-I data are statistically limited at high Q^2 and the much higher HERA-II luminosity improves the measurement in this region.

A preliminary combination of the HERA-I and high Q^2 HERA-II data has been made [3] and a new set of measurements for each process, NC and CC, from e^+p and e^-p interactions has been obtained. Figure 1 shows the combined HERA-I data (top) and first preliminary result on combined HERA-I and high Q^2 HERA-II data (bottom) for NC $e^{\pm}p$ cross sections. From this figure one can see that the addition of the HERA-II data significantly improves precision at high x and Q^2. The HERAPFD1.0 and HERAPDF1.5 [4] fits are superimposed on the data (more details about HERAPDF1.5 in section 4). The influence of the structure function xF_3 is clearly visible at large Q^2.

The combination will be updated when H1 and ZEUS publish all their individual measurements of DIS at high Q^2. H1 has recently presented its measurement of inclusive NC and CC cross sections with the full HERA-I and HERA-II data samples at $\sqrt{s}$ =319 GeV [5].

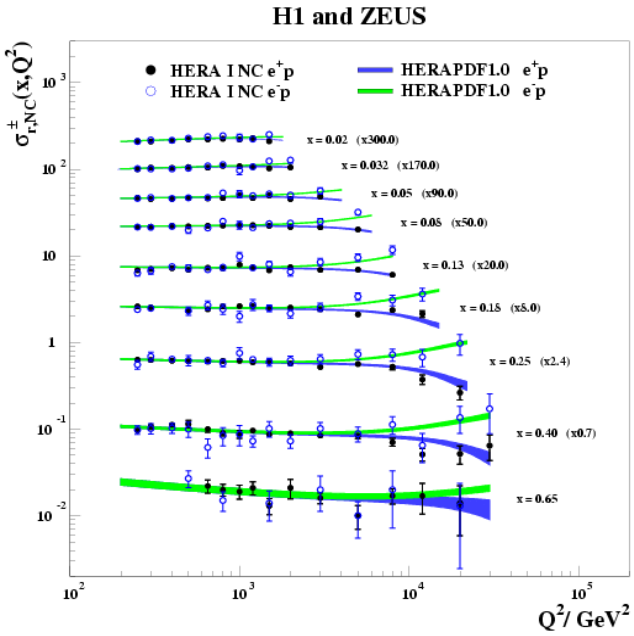

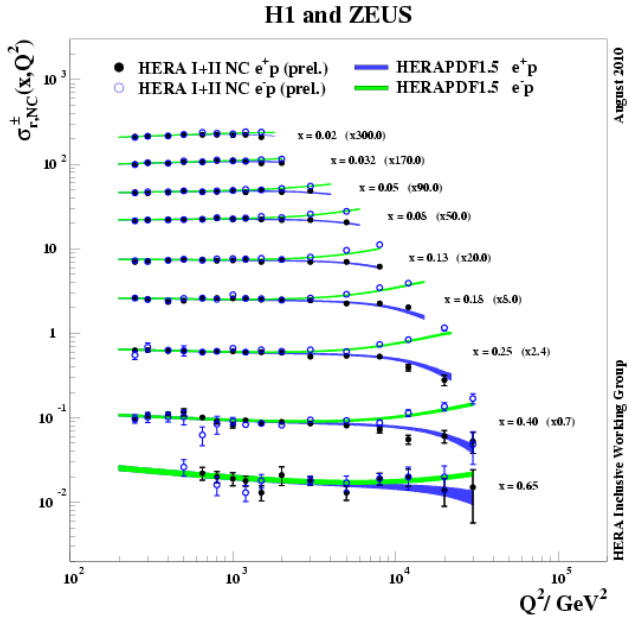

Fig. 1 – NC $e^{\pm}p$ cross sections as a function of Q^2 in bins of x, for combined data from HERA-I period (top) and combined data from HERA-I with addition of high Q^2 data from HERA-II period (bottom). The PDF fits to this data, HERAPDF1.0 (top) and HERAPDF1.5 (bottom) are superimposed. The bands represent the total uncertainty of the fit.

3.2. F_L

At low x, NLO QCD in the DGLAP formalism predicts that the longitudinal structure function is strongly related to the gluon PDF at low x values.

In the final running period in 2007, the proton beam was accelerated to three different beam energies (920, 575, 460 GeV) and NC e^+p data were collected. These data access high y and have been used to measure the longitudinal structure function F_L [6,7,8]. The reduced cross section measurements with H1 and ZEUS data from these runs have been combined and the structure function F_L extracted [9]. Recall that the NC e^+p reduced cross section is given by $\sigma_r = F_2 - y^2F_L/Y_+$, for $Q^2 << M_Z^2$. Since $Q^2 = sxy$ one needs measurements at different s values in order to access different y values for the same x,Q^2 point. The structure function F_L is measured as a slope of a linear fit of σ_r *versus* $f(y) = y^2/Y_+$, in x,Q^2 bins. The measured F_L averaged in x as a function of Q^2 is shown in Fig. 2, with various theoretical predictions superimposed.

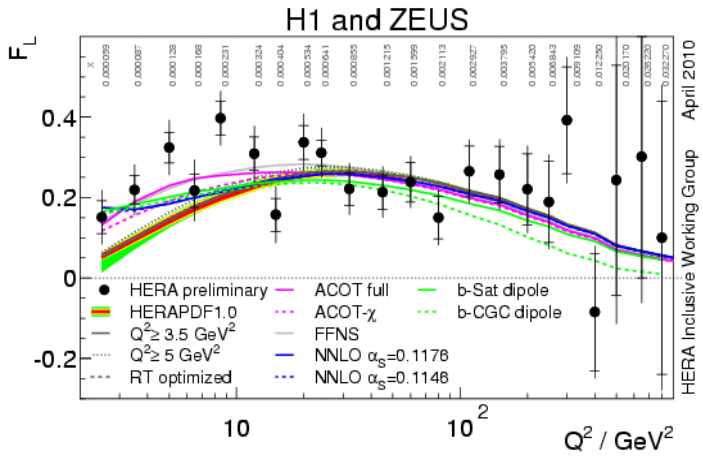

Fig. 2 – The HERA combined measurement of F_L averaged in x at a given value of Q^2 with various theoretical predictions superimposed. The inner (full) error bars on the data points represent the statistical (total) uncertainties.

3.3. $F_2^{c\bar{c}}$ and $F_2^{b\bar{b}}$

The charm and beauty production are studied at HERA *via* neutral current scattering. Heavy flavor quarks are predominantly produced by the boson-gluon fusion process, $\gamma g \to c\bar{c}$, which is sensitive to the gluon distribution in the proton. According to equation (1), the cross section may then be written in terms of the structure functions $F_2^{c\bar{c}}$ and $F_2^{b\bar{b}}$ when the virtuality of the exchanged boson is small, $Q^2 << M_Z^2$.

A preliminary combination has been made of data on $F_2^{c\bar{c}}$ [10] from various different methods of tagging charm: using the D*$^{\pm}$ meson production, using the vertex detectors for the displaced decay vertex, using direct D^0, D^+ production, and indentifying semi-leptonic charm decays *via* muons. The results of the $F_2^{c\bar{c}}$ combination compared to the separate measurements which went into it are shown in Fig. 3. The combined data show a considerable improvement in precision. This combination will be updated to include the recently obtained new results on $F_2^{c\bar{c}}$ from H1 [11] and ZEUS [12]. Data on $F_2^{b\bar{b}}$ have not yet been combined.

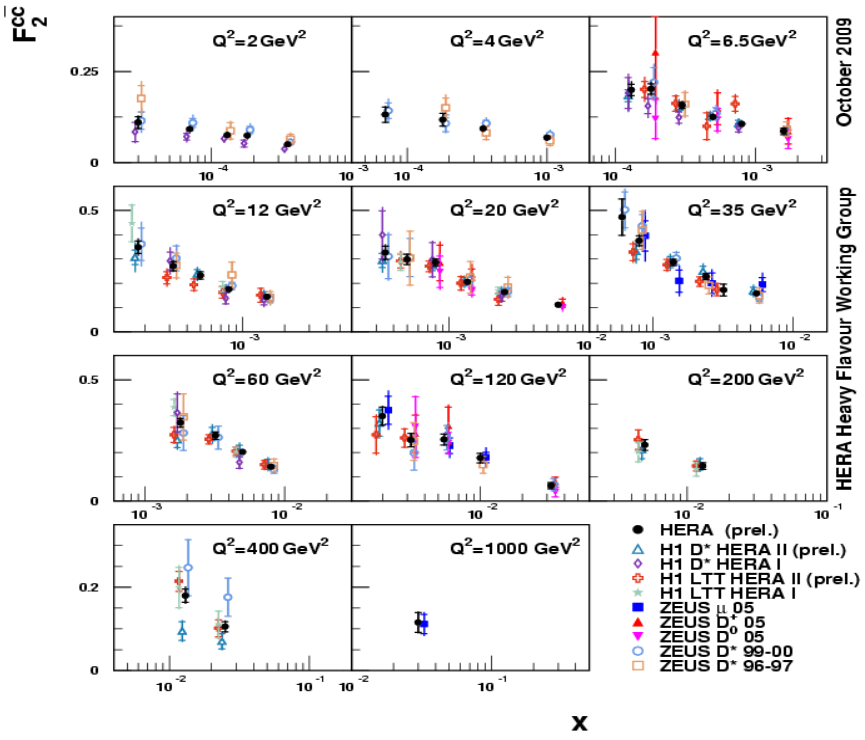

Fig. 3 – The HERA combined measurement of $F_2^{c\bar{c}}$ compared to the data sets of H1 and ZEUS used for the combination. The inner (full) error bars of the averaged value represent the uncorrelated (total) uncertainties. These data sets are slightly displaced in x for better visibility.

4. PDFS FROM COMBINED MEASUEREMENTS

The general approach to determine the PDFs from experimental DIS cross section measurements consists of several steps. First, the PDFs are parameterised at a low starting scale Q_0^2 by smooth analytical functions with few free parameters. After this, these functions are evolved using the DGLAP equations to higher Q^2 values and calculations of the structure functions and the cross sections are performed. The calculations are compared to experimental data and minimisation of the χ^2 is performed adjusting the free parameters. Several constraints can be applied, like momentum sum rules, requiring the known quark flavor numbers of the proton and possibly a few more.

The combined HERA-I and high Q^2 HERA-II data sets are used as the sole input to a PDF fit termed HERAPDF1.5 [4] which uses the same formalism and assumptions as the HERAPDF1.0 fit. The x dependence of PDFs for Q^2 = 10 GeV^2

from HERAPDF1.0 and HERAPDF1.5 are shown in Fig. 4. Each of the plots from Fig. 4 is a summary plot for the valence distributions for up and down quarks as well as the gluon and sea quark distributions which are scaled down by a factor of 20. The errors including the experimental, model and the PDF parameterisation uncertainties are also shown. The χ^2 per degree of freedom of the HERAPDF1.0 is 576/592 and for HERAPDF1.5 967/1032. From Fig. 4 one can see that the combination with the HERA-II data provides an improvement particularly at high x in the valence sector.

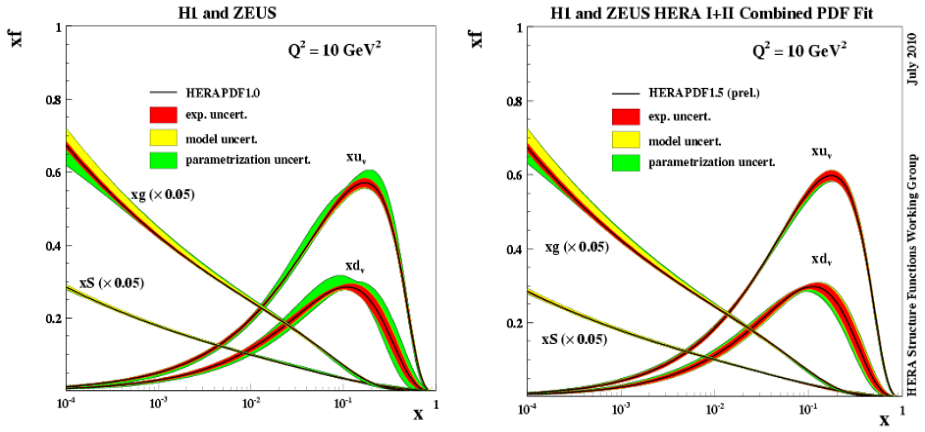

Fig. 4 – The x dependence of the parton density functions from HERAPDF1.0 (left) and HERAPDF1.5 (right) for: xu_v, xd_v, $xS = x(\overline{U} + \overline{D})$ and xg at $Q^2 = 10$ GeV^2. The errors including the experimental, model and the PDF parameterisation uncertainties are also shown in the plots.

The combined $F_2^{c\bar{c}}$ data can help to reduce the uncertainty on PDFs coming from the choice of heavy quark scheme and the value of the charm mass parameter input to these schemes [13]. The left panel of Fig. 5 compares the χ^2, as a function of the charm mass parameter, for a fit which includes charm data for various heavy-quark schemes. Each of these schemes favors a different value for the charm quark mass parameter, and the fit to the data is good for all the heavy quark mass schemes except for the zero-mass scheme. Predictions for W and Z production at the LHC are sensitive to the value of the charm mass parameter and to the heavy quark scheme used, as shown in the right panel of Fig. 5. For any chosen value of the charm mass the spread of predictions for different schemes is about 7%. However this spread is considerably reduced to about 1% if each heavy quark scheme is used at its own favoured value of the charm quark mass.

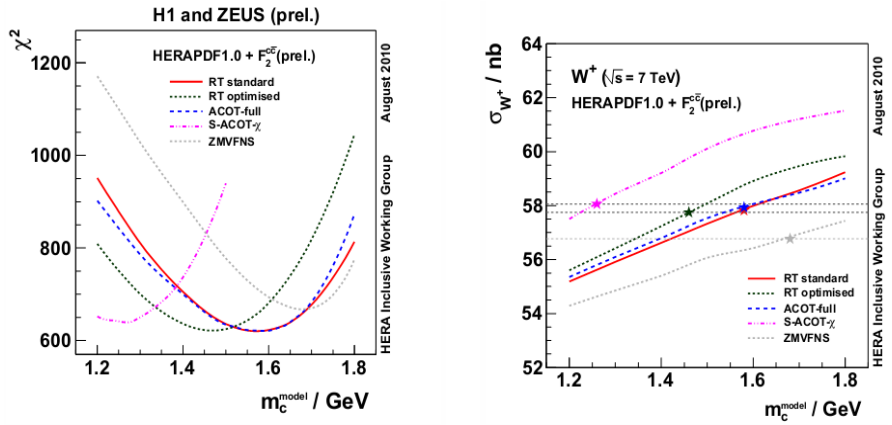

Fig. 5 – For various heavy-quark schemes. Left: the χ^2 of the HERAPDF fit as a function of the charm mass parameter when $F_2^{c\bar{c}}$ data are included. Right: predictions for W^+ cross sections at the LHC as a function of the charm mass parameter. The star marks the optimal value of the charm mass parameter in each scheme.

Measurements of jet cross sections can provide a direct determination of the gluon density since the QCD processes that give rise to scaling violations in the inclusive cross sections, namely the QCD-Compton and boson-gluon-fusion processes, can also be observed as events with distinct jets in the final state. So far H1 and ZEUS jet data have not been combined but some separate H1 and ZEUS jet data sets [14,15,16,17] have been input to the HERAPDF1.6 NLO QCD fit [18] in order to exploit their ability to constrain the gluon PDF and to make a determination of the value of the strong coupling constant $\alpha_s(M_Z)$ simultaneously with the PDF determination. HERAPDF1.6 uses the same combined H1 and ZEUS inclusive DIS measurements as the HERAPDF1.5 fit. The left hand side of Fig. 6 shows HERAPDF1.5f [18] which uses the same input as HERAPDF1.5 but with a more flexible parameterisation and treating $\alpha_s(M_Z)$ as a free parameter, as in HERAPDF1.6. Due to the free $\alpha_s(M_Z)$, the uncertainty of the gluon PDF is much larger than for HERAPDF1.5 (Fig. 4 right). As expected, the gluon distribution is significantly improved when using the jet data in HERAPDF1.6 (Fig. 6 right).

The most recent NLO QCD analysis performed with HERA data [19] includes the following data sets: the NC and CC inclusive DIS cross sections obtained from the combination of the measurements from H1 and ZEUS based on HERA-I and HERA-II data at the nominal proton beam energy, the preliminary combined inclusive NC DIS cross sections at reduced proton beam energies, the inclusive jet cross sections from H1 and ZEUS and the preliminary combined

HERA results on the structure function $F_2^{c\bar{c}}$. This fit, termed HERAPDF1.7, shows that the different cross sections measured at HERA give consistent information on the proton PDFs.

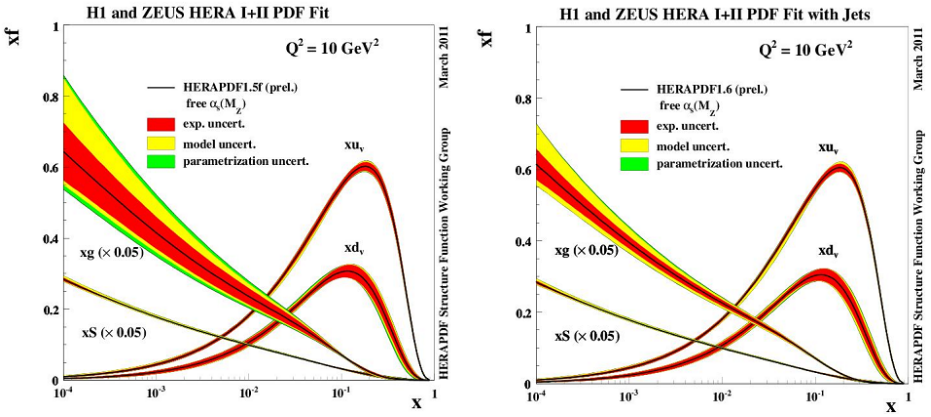

Fig. 6 – Parton density functions from HERAPDF1.5f (left) and HERAPDF1.6 (right) for: xu_v, xd_v $xS = x(\bar{U} + \bar{D})$ and xg at Q^2 = 10 GeV^2. The errors including the experimental, model and the PDF parameterisation uncertainties are also shown in the plots.

So far HERAPDFs successfully describe both Tevatron and LHC data on W, Z and jet production. Figure 7 shows a comparison of the HERAPDF1.5 NLO predictions to the early LHC data on the W asymmetry from the CMS experiment.

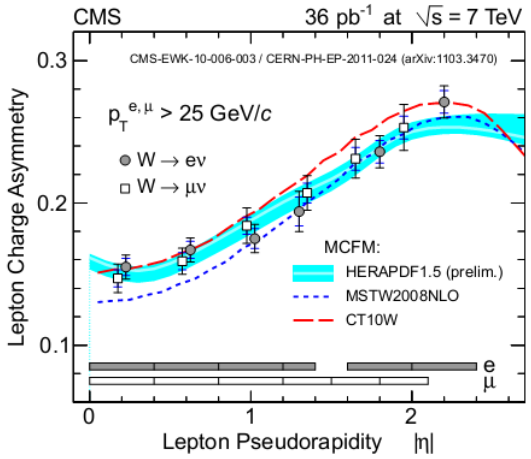

Fig. 7 – W decay lepton asymmetry data from CMS compared with predictions based on HERAPDF1.5 NLO and other PDF sets.

5. CONCLUSIONS

The inclusion of new data sets from HERA-II running period, in the analysis of deep inelastic $e^{\pm}p$ scattering, has provided new information on PDFs. Inclusive data at high Q^2 provide an improvement on the precision of PDFs at high x and Q^2 values. The combination of data measured at reduced proton beam energy provides an improvement of the measurement of the longitudinal structure function which is directly related to the gluon PDF at small x. The addition of charm data provide important information on heavy quark schemes and the charm quark mass parameter used in PDF fit. The jet data which so far are used separately from H1 and ZEUS, provide an improvement of the precision of the gluon PDF and independent information on $\alpha_s(M_Z)$.

The H1 and ZEUS collaborations are working on finalising their individual analyses as well as combining their results to obtain the optimal precision.

Acknowledgments. The results presented here are obtained from the combined efforts of many colleagues from H1 and ZEUS Collaborations and I thank all of them.

REFERENCES

1. V.N. Gribov and L.N. Lipatov, Sov. J. Nucl. Phys., **15**, 438 (1972),
   V.N. Gribov and L.N. Lipatov, Sov. J. Nucl. Phys., **15,** 675 (1972),
   Y.L. Dokshitzer, Sov. Phys. JETP, **46**, 641 (1977),
   G. Altarelli and G. Parisi, Nucl. Phys., **B 126**, 298 (1977).
2. F.D.Aaron et al. (H1 Collaboration), JHEP, **01** 109, (2010).
3. H1 and ZEUS Collaborations, H1prelim-10-141, ZEUS-prel-10-017.
4. H1 and ZEUS Collaborations, H1prelim-10-142, ZEUS-prel-10-018.
5. F.D.Aaron et. al,, H1 Collaboration, DESY 12-107.
6. F.D.Aaron et. al,, (H1 Collaboration), Phys. Lett., **B 665**, 139 (2008).
7. S. Chekanov et al., (ZEUS Collaboration), Phys. Lett., **B 682**, 8 (2009).
8. F.D. Aaron et al. (H1 Collaboration), Eur. Phys. J., **C 71**, 1579 (2011).
9. H1 and ZEUS Collaborations, H1prelim-10-044, ZEUS-prel-10-008.
10. H1 and ZEUS Collaborations, H1prelim-09-171, ZEUS-prel-09-015.
11. D. Aaron et al. (H1 Collaboration), Eur. Phys. J., **C 71**, 1769 (2011).
12. ZEUS Collaboration, ZEUS-prel-12-002.
13. H1 and ZEUS Collaborations, H1prelim-10-143, ZEUS-prel-10-019.
14. F.D. Aaron et al. (H1 Collaboration), Eur. Phys. J., **C 65**, 363 (2010).
15. F.D. Aaron et al. (H1 Collaboration), Eur. Phys. J., **C 67**, 1 (2010)
16. S. Chekanov et al. (ZEUS Collaboration), Phys. Lett., **B 547**, 164 (2002).
17. S. Chekanov et al. (ZEUS Collaboration), Nucl. Phys., **B 765**, 1 (2007).
18. H1 and ZEUS Collaborations, H1prelim-11-034, ZEUS-prel-11-001
19. H1 and ZEUS Collaborations, H1prelim-11-143, ZEUS-prel-11-010.